Scientific Report for Loan 914:

Interaction of Tectonics and Magmatism in the Askja and Krafla Spreading Segments of Iceland

Prof. Robert S. White (rsw1@cam.ac.uk), Jon Tarasewicz, Tim Greenfield & Rob Green

September 2013

Abstract

This loan comprised 40 SEIS-UK seismometers operating alongside 10 Cambridge-owned seismometers to provide coverage of 150 km of the Northern Volcanic Zone (NVZ) active spreading centre in Iceland, with denser local arrays around Askja and Krafla volcanoes, during July 2010 – September 2011 (Fig. 1). The loan of 30 SEIS-UK seismometers was extended to September 2012 to enable monitoring of increased seismic activity under Vatnajökull at the south end of the NVZ. We purchased a further 15 seismometers using NERC funding, thus maintaining a network of 55 instruments during the extension period. The work was supported by a NERC research grant and NERC post-doc and Ph.D studentships as well as several M.Sci. research projects. Preliminary results include: mapping of several thousand earthquakes along the rift zone in both the lower and upper crust; tomographic evidence for the magma chamber under Askja; detailed analysis of how strike-slip faulting accommodates shear in the transfer zone between rift segments; evidence for strongly non-double-couple source mechanisms at Krafla; demonstration of faulting in the brittle layer at extremely low stress drops of 1–3 bars, probably caused by migration of carbon dioxide from an underlying magmatic intrusion.

Background

The Northern Volcanic Zone (NVZ) of Iceland is persistently seismically active, ultimately due to spreading of ~2 cm/yr being accommodated across its rift segments. However, the permanent monitoring network of the Icelandic Meteorological Office (IMO) is relatively sparse in the NVZ. Our network has provided far denser coverage around Askja (last eruption 1961) and Krafla (last eruption episode 1975–1984) volcanoes, with additional stations along the length of the NVZ beyond and between these two most recently active volcanic centres (Fig. 1). Increased activity under Vatnajökull, at the southern end of the network, is of particular interest because several sub-glacial volcanoes there have the potential to form both hazardous *jökulhlaups* (glacial floods) and ash-rich plumes as a result of ice-magma interaction,

exemplified by Eyjafjallajökull volcano in 2010. Monitoring and understanding the magmatic plumbing systems of Askja (which erupted explosively in 1875 with catastrophic consequences for much of east Iceland) and Krafla (which has a significant commercial geothermal power plant operating in its caldera) remains very important.

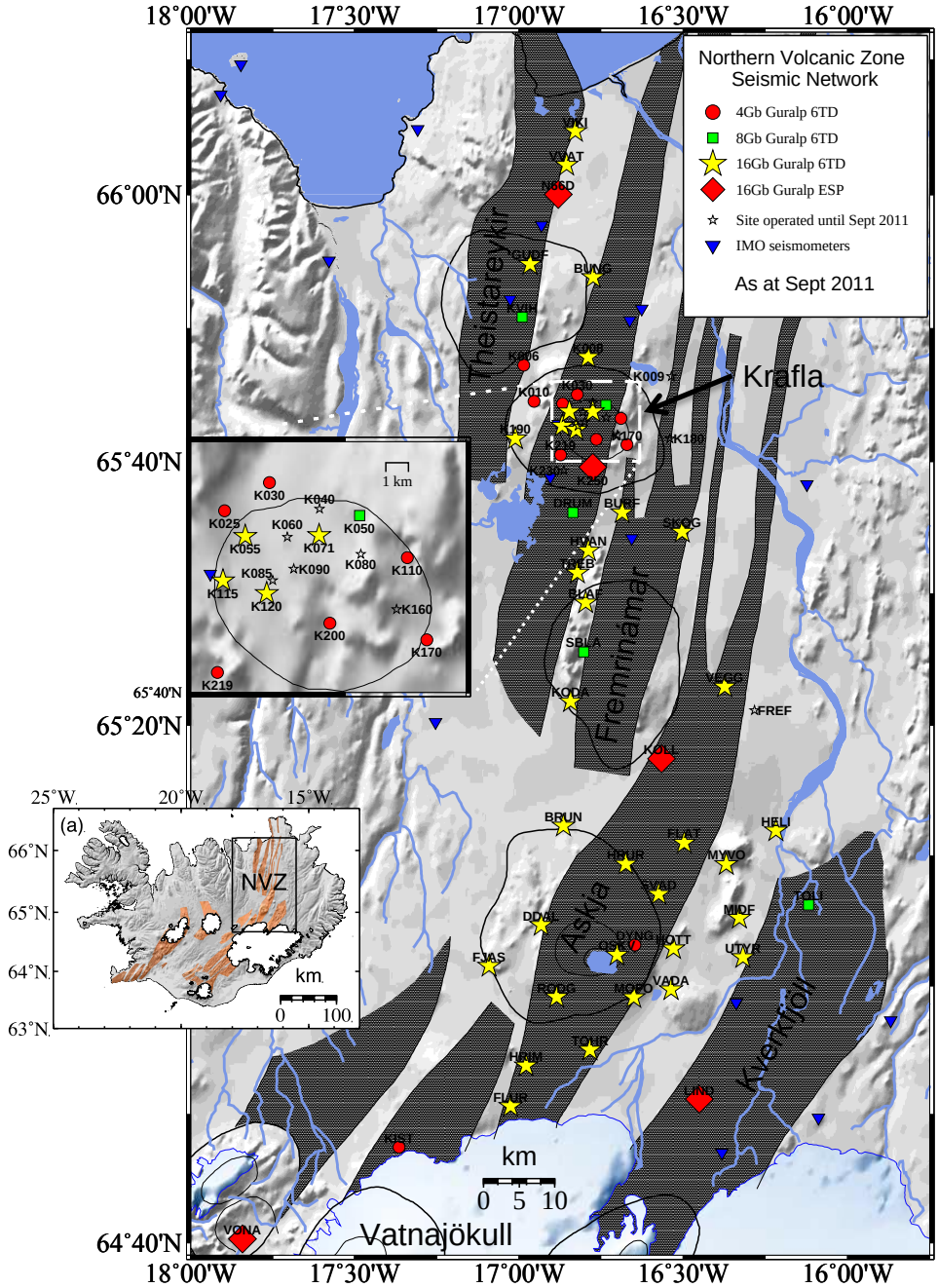

FIGURE 1: *Network location map for September 2011 – July 2012 during the second year of Loan 914. Sites also operated July–Sept 2011 (maximum network size) are shown by small black stars. Inset (a) shows location of main map. Top inset shows Krafla caldera. Grey-shaded zones show fissure swarms associated with volcanoes (labelled) in the NVZ. See Appendix for exact station locations.*

Survey procedure

Loan 914 aggregated instruments that were already deployed in Iceland under Loans 857 (15x 16 Gb Güralp 6TDs around Askja) and 891 (15x 8 Gb 6TDs around Krafla caldera). Additional to these 30 instruments, ten more 16 Gb 6TDs were deployed in July 2010 under Loan 914. Ten Cambridge-owned 4 Gb instruments were also already in the field, giving a total network of 50 instruments in July 2010. In July 2011, we deployed 10 new Cambridge-owned 16 Gb 6TDs and five 16 Gb ESPDs (network total = 65 instruments). Subsequently, in September 2011, we returned 10 SEIS-UK 6TDs (8 Gb), whilst 30 SEIS-UK 6TDs and all Cambridge-owned instruments remained deployed under the Loan 914 extension (network total = 55 instruments). The Loan 914 period ended in September 2012. The network was serviced in July/August 2010, March (Krafla only)/July/September 2011, and April (Askja only)/July 2012, with some redistribution of stations in July/September 2011 and July 2012. Station locations are given in the Appendix and Figure 1.

Seismometers were either buried directly in soil or on cement plinths inside barrel vaults. We recorded at 100 or 200 samples per second (sps) during the shorter summer service interval, and 50 sps over winter, which allowed us to record continuously all year without exceeding the 16 Gb sensors' memory capacity. Stations were powered by a combination of solar panels (≥120 W for sites expected to run all winter), batteries (≥230 Ah, often ≥345 Ah) and, in some cases, wind turbines. Use of wind turbines was only partly successful due to ice accumulation and very strong winds during the Icelandic winter. Nevertheless, power loss over winter was limited by the generous use of batteries and solar panels, which were mounted on wooden A-frames at least 50 cm above the surface. Equipment failure was minimised compared to previous campaigns by mounting breakout boxes on stakes above ground such that they did not become waterlogged and frozen in ice.

Data quality

The majority of local events recorded in the NVZ are of only small magnitudes ($M_L < 2$). Nonetheless, many local events have clear P- and S-wave arrivals (Fig. 2), and regional events of $M_L \geq 2$ can be observed across the entire network along the length of the NVZ.

Processing and modelling

Data were quality controlled in the field and converted to miniseed format using SEIS-UK standard procedures. An initial catalogue of automatic earthquake locations has been obtained using Coalescence Microseismic Mapping (CMM) software (Drew *et al.*, 2013). We have refined earthquake locations using manual P- and S-wave arrival picks and investigated source mechanisms using P-wave first-motion polarities and P/S amplitude ratios for simple double-couple source inversions as well as full moment tensor solutions (Green *et al.*, in press; Watson *et al.*, in prep.). Manual P- and S-wave arrival time picks have been used to carry out tomography around Askja (Mitchell *et al.*, 2013).

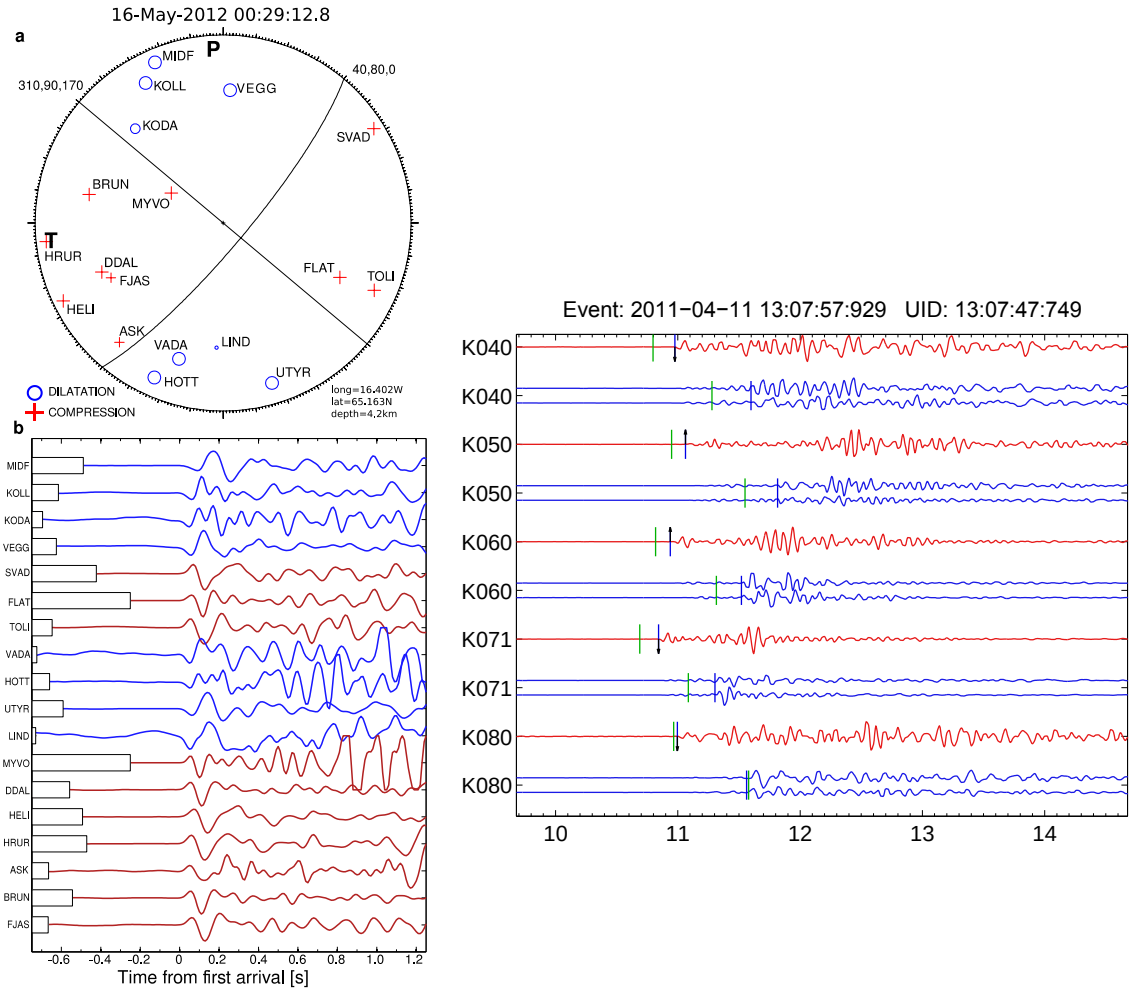

FIGURE 2: *Data examples. (Left) Event recorded in the transform zone between Askja and Kverkfjöll rift segments, with vertical component traces and picked P-wave first-motion polarities aligned on the first arrival (from Green et al., in press). (Right) Example vertical (red) and horizontal (blue) component traces recorded on stations in Krafla caldera.*

Preliminary findings

During the loan period, the network has recorded several thousand events at Krafla and Askja, including deep crustal events (Fig. 3). At Krafla, all well-constrained earthquakes are shallow (< 4 km) and coincide spatially with the location of either geothermal fields associated with the power station in the caldera, or are located above, or close to, the putative magma chamber. At Askja, most activity is also at relatively shallow levels, above the brittle-ductile transition (~6–7 km), but we also observe much deeper activity in the normally ductile mid- and lower crust which we attribute to melt movement.

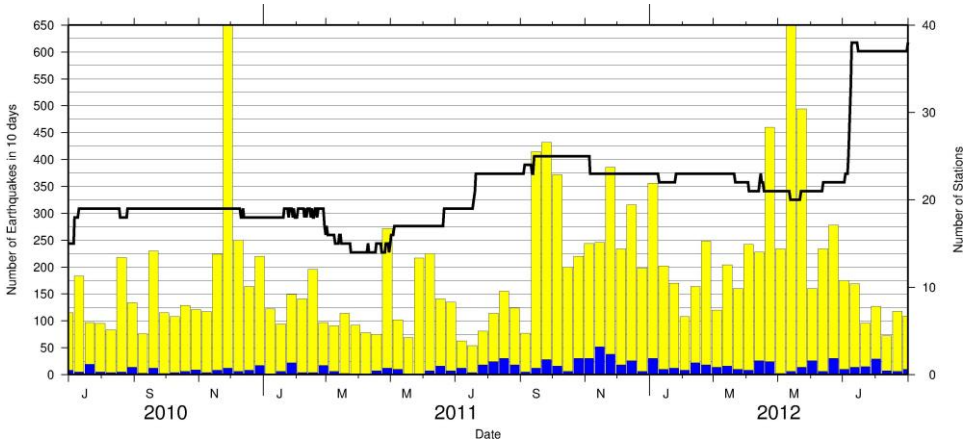

FIGURE 3: *Histogram of earthquakes detected in the south part of the network around Askja (yellow <10 km deep; blue >10 km deep). Black line (scale right) shows number of stations operating at the time (only for the Askja part of the network).*

Interpretation to date

We interpret all of the seismicity deeper than approximately 8 km as being associated with magma migration and intrusion in the crust (Key *et al.*, 2011; White *et al.*, 2011; White *et al.*, 2012), where the high strain rates cause brittle failure in otherwise ductile crust. Shallower earthquakes are likely due to hydrothermal fluid circulation driven by heat from magma chambers, geothermal exploitation and tectonic stresses across the rift zone. Preliminary tomographic results suggest that there is a magma chamber at ~6–8 km depth beneath Askja (Fig. 4; Mitchell *et al.*, 2013). We have found evidence (in the earthquake distribution and fault-plane solutions) for spreading being accommodated by bookshelf faulting in the transfer zone between the Askja and Kverkfjöll rift segments (Fig. 5; Green *et al.*, in press). At Krafla, we observe well-constrained, strongly non-double-couple earthquakes that we interpret as being associated with the evacuation and collapse of fluid-filled cavities (Watson *et al.*, in

prep.). Stress modelling and the timing of earthquakes around a mid-crustal dyke intrusion at Upptyppingar (Fig. 4) suggest that subsequent, shallower earthquakes are triggered by volatiles that have exsolved from the magma in the mid-crustal dyke (Martens & White, 2013).

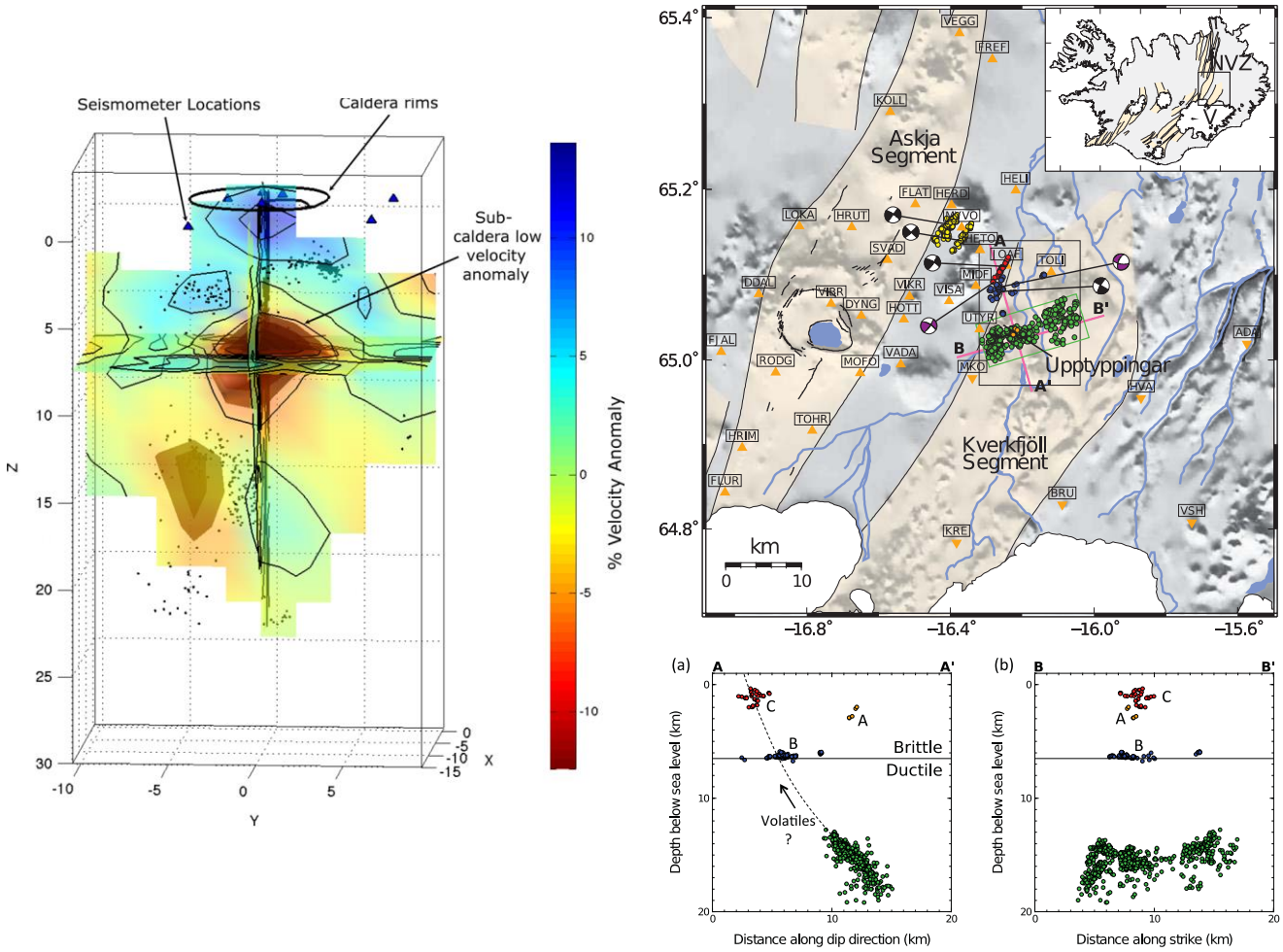

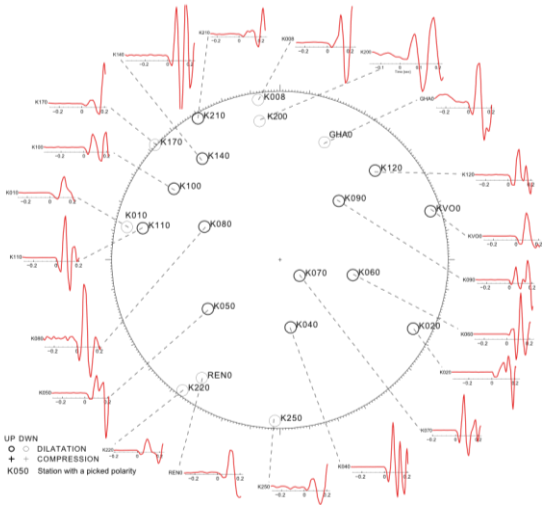

FIGURE 4: ***Top left:*** *Tomographic image of P-wave velocity variation beneath Askja volcano (Mitchell et al., in press).* ***Top right****: Map and cross-sections of seismicity caused by a dyke intrusion (green dots) and subsequent triggered earthquakes in the upper crust (clusters A, B, C) (Martens & White, 2013).* ***Bottom right:*** *P-arrival waveforms and lower-hemisphere projection of station locations for a strongly non-double-couple (implosive) event at Krafla (Watson et al., in prep.)*

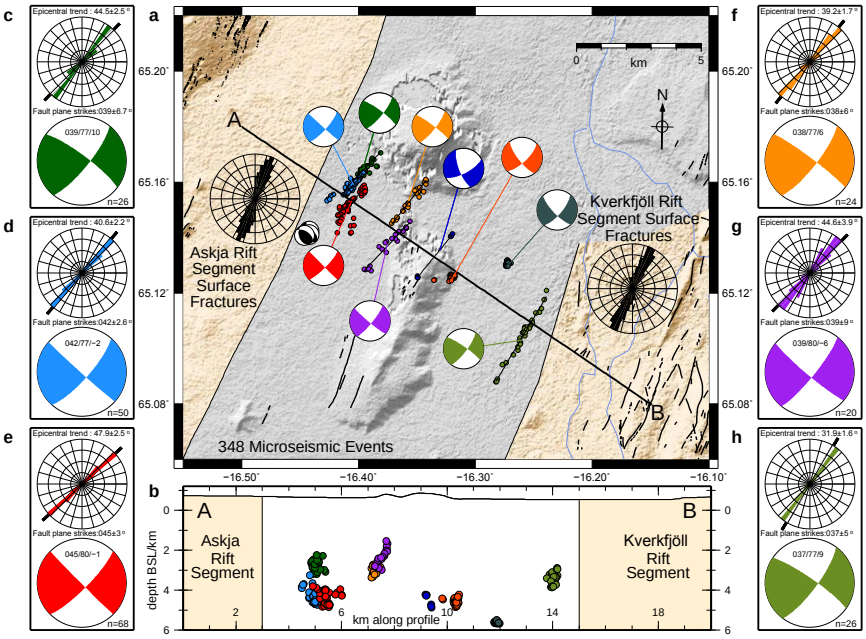

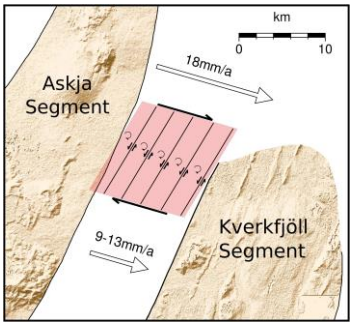

FIGURE 5: ***Top****: Hypocentre locations and fault-plane solutions for earthquakes on NNE-SSW-striking faults that accommodate shear in the transform zone between Askja and Kverkfjöll rift segments.* ***Right****: Cartoon illustrating shear and rotation of blocks in the transform zone between the volcanic rift segments (Green et al., in press).*

Conclusions and Recommendations

The network deployed along the NVZ with a focus on Askja and Krafla volcanoes has enabled a significantly lower detection threshold than the permanent national monitoring network operated by the IMO. The dense array has facilitated detailed analysis of earthquake locations, tomography and source mechanisms, thus allowing us to image magmatic intrusions and speculate on source processes and the relationship between magmatism and the seismicity we have recorded. The rich dataset acquired under Loan 914 is the subject of ongoing study, including denser travel time tomography around Askja and Krafla, investigation of anisotropy caused by cracks in the upper crust and in the Krafla geothermal area, regional crustal velocity structure control by ambient noise analysis, receiver function analyses of Moho and mantle discontinuities, ongoing temporal changes in seismicity caused by the 2007 Upptyppingar intrusion, and the use of regional earthquakes for crustal structure studies along the NVZ.

Publications

Green. R. G., White. R. S., Greenfield. T. (2013), Motion in the north Iceland rift zone accommodated by bookshelf faulting. *Nature Geoscience*, in press. (Loan 914).

Key, J., White, R. S., Soosalu, H. & Jakobsdóttir, S. S. (2011). Multiple melt injection along a spreading segment at Askja, Iceland. *Geophysical Research Letters*, **38**, L05301, doi:10.1029/2010GL046264 (Loans 842, 857 & 914)

Key, J., White, R. S., Soosalu, H. & Jakobsdóttir, S. S. (2011). Correction to "Multiple melt injection along a spreading segment at Askja, Iceland", *Geophysical Research Letters*, **38**, L10308, doi:10.1029/2011GL047491 (Loans 842, 857 & 914)

Martens, H. R. & White, R. S. (2013). Triggering of microearthquakes in Iceland by volatiles released from a dyke intrusion, *Geophysical Journal International*, **194 (3),** 1738–1754, doi: 10.1093/gji/ggt184 (Loan 914)

Mitchell, M., White, R. S., Roecker, S. & Greenfield, T. Tomographic image of melt storage beneath Askja volcano, Iceland using local microseismicity, *Geophysical Research Letters*, in press. (Loans 857 & 914)

Soosalu, Heidi, Key, Janet & White, Robert S. (2011), Laatikollisesta varaseismometrejä rift-alueen alakuoren synnyn jäljille, [From a box of spares to tracking down lower crust generation at a rift], *Geologi*, **63**, 36–43. (Loans 842, 857 & 914)

Watson, Z., Tarasewicz, J., Pugh, D., White, R. S. and Brandsdóttir, B., (in prep.), Non-double-couple earthquakes at Krafla volcano, Iceland, *Geophysical J. Int.*, (Loans 891 & 914)

White, Robert S., Redfern, Simon A. T. & Chien, Su-Ying (2012). Episodicity of seismicity accompanying melt intrusion into the crust, *Geophysical Research Letters*, **39**, L08306, doi:10.1029/2012GL051392 (Loan 914)

Dissertations

Green, Robert (2012) Swarm microseismicity and upper crustal faulting between the Askja and Kverkfjöll volcanic systems, Iceland M.Sci. dissertation, University of Cambridge, U.K. (Loan 914).

Greenfield, T. (2011), Microseismicity of the Krafla Volcanic System, Iceland, M.Sci. dissertation, University of Cambridge, U.K. (Loan 914).

Key, Janet (2011) Tracking melt with lower crustal earthquakes at Askja, Iceland, PhD Dissertation, University of Cambridge, U.K. (Loans 842, 857 & 914)

Mitchell, Michael (2011) 3-D Tomographic Inversion of Local Microseismic Events to Image the Askja Magma Chamber, M.Phil. dissertation, University of Cambridge, U.K. (Loans 842, 857 & 914)

Watson, Z. (2013), Microseismicity within the Krafla Caldera, NE Iceland, M.Sci. dissertation, University of Cambridge, U.K. (Loans 891 & 914)

Conferences (25 abstracts) Work based on Loan 914 has also been presented at:
American Geophysical Union Conference, San Francisco, USA, 2012; 2013;
Magmatic Rifting and Active Volcanism Conference, Addis Ababa, January 2012;
Volcanic and Magmatic Studies Group, Cambridge, 2011; Bristol 2013;
British Geophysical Association Conference, Cambridge, U. K., Sept 2013;
AGU Chapman Conference, Hawaii, 2012;
European Seismological Commission, Salina 2011; El Hierro 2012; Sulawesi 2013;
EGU General Assembly, Vienna, 2011.

APPENDIX: Instrument deployment details

Northern Volcanic Zone Network (July 2010 to July 2011)

Station	Latitude (º)	Longitude (º)	Elevation (m)	Capacity (Gb)*
VIKI	66.07812	-16.82937	58	16
GUDF	65.91337	-16.96684	321	16
BUNG	65.89703	-16.77482	449	16
K008	65.79724	-16.79029	507	8
K006	65.78729	-16.98611	408	4
K009	65.77358	-16.53669	356	8
K030	65.75034	-16.82364	526	4
K010	65.74187	-16.95551	433	4
K040	65.73993	-16.77539	560	8
K050	65.73723	-16.73658	631	8
K071	65.72937	-16.77582	552	8
K060	65.72869	-16.80646	547	8
K080	65.72184	-16.73532	637	8
K110	65.72048	-16.69025	613	8
K090	65.71597	-16.80041	542	8
K120	65.70619	-16.82666	519	8
K160	65.69981	-16.70053	556	8
K180	65.69549	-16.54101	421	4
K190	65.69505	-17.01160	393	4
K200	65.69435	-16.76543	474	8
K170	65.68755	-16.67146	530	4
K219	65.67458	-16.87433	463	4
K250	65.65915	-16.77652	378	4
K230	65.65517	-16.86379	387	4
DRUM	65.60223	-16.83693	384	8
BURF	65.60217	-16.68633	382	16
SKOG	65.57792	-16.50440	402	16
HVAN	65.55409	-16.78980	349	8
BLAF	65.48870	-16.79785	644	16
VEGG	65.38205	-16.37467	507	16
KODA	65.36317	-16.84383	517	16
FREF	65.35190	-16.28355	533	16
KOLL	65.29024	-16.56726	593	16
HELI	65.19875	-16.21843	491	16
FLAT	65.18279	-16.49796	728	16
HRUR	65.15577	-16.67551	697	16
MYVO	65.15550	-16.36895	639	16
SVAD	65.11746	-16.57498	680	16
TOLI	65.10336	-16.11953	537	8
MIDF	65.08676	-16.32961	572	16
DDAL	65.07739	-16.93341	801	16
DYNG (ask)	65.05192	-16.64819	955	4
HOTT	65.04748	-16.52985	718	16
UTYR	65.03605	-16.31867	623	16
VADA	64.99487	-16.53817	673	16
RODG	64.98513	-16.88639	1022	16
MOFO	64.98440	-16.65119	702	16
TOHR	64.91658	-16.78473	715	16
HRIM	64.89633	-16.97921	849	16
FLUR	64.84354	-17.02693	838	16

*** 4 Gb sensors are Cambridge-owned; all others SEIS-UK Loan 914**

Northern Volcanic Zone Network (July 2011 to Sept 2011)

Station	Latitude (º)	Longitude (º)	Elevation (m)	Capacity (Gb)
VIKI	66.07812	-16.82937	58	16
VVAT	66.03643	-16.85612	132	16
N66D	66.00009	-16.88126	200	16
GUDF	65.91337	-16.96684	321	16
BUNG	65.89703	-16.77482	449	16
KVIH	65.84712	-16.99152	351	8
K006	65.78729	-16.98611	408	4
K008	65.79724	-16.79029	507	16
K009	65.77358	-16.53669	356	8
K010	65.74187	-16.95551	433	4
K025	65.73909	-16.86740	523	4
K030	65.75034	-16.82364	526	4
K040	65.73993	-16.77539	560	8
K050	65.73723	-16.73658	631	8
K055	65.72894	-16.84718	549	16
K060	65.72869	-16.80646	547	8
K071	65.72937	-16.77582	552	16
K080	65.72184	-16.73532	637	8
K085	65.71133	-16.82091	523	16
K090	65.71597	-16.80041	542	8
K110	65.72048	-16.69025	613	8
K115	65.71123	-16.86879	544	16
K120	65.70619	-16.82666	519	8
K160	65.69981	-16.70053	556	8
K170	65.68755	-16.67146	530	4
K180	65.69549	-16.54101	421	4
K190	65.69505	-17.01160	393	4
K200	65.69435	-16.76543	474	8
K219	65.67458	-16.87433	463	4
K230	65.65517	-16.86379	387	4
K250	65.65915	-16.77652	378	16
DRUM	65.60223	-16.83693	384	8
BURF	65.60217	-16.68633	382	16
SKOG	65.57792	-16.50440	402	16
HVAN	65.55409	-16.78980	349	16
TREB	65.52641	-16.82279	450	16
BLAF	65.48870	-16.79785	644	16
SBLA	65.42633	-16.80327	646	8
KODA	65.36317	-16.84383	517	16
BRUN	65.20461	-16.86597	536	16
DYNG (ask)	65.05194	-16.64806	955	4
DDAL	65.07739	-16.93341	801	16
FJAS	65.02470	-17.09217	798	16
FLAT	65.18279	-16.49796	728	16
FLUR	64.84354	-17.02693	838	16
FREF	65.35190	-16.28355	533	16
HELI	65.19875	-16.21843	491	16
HOTT	65.04748	-16.52985	718	16
HRIM	64.89633	-16.97921	849	16
HRUR	65.15577	-16.67551	697	16
KOLL	65.29024	-16.56726	593	16
LIND	64.85278	-16.45230	726	16
MIDF	65.08676	-16.32961	572	16
MOFO	64.98440	-16.65119	702	16
MYVO	65.15550	-16.36895	639	16
OSKV	65.03933	-16.70164	1209	16
RODG	64.98513	-16.88639	1022	16
SVAD	65.11746	-16.57498	680	16
TOHR	64.91658	-16.78473	715	16
TOLI	65.10336	-16.11953	537	8
UTYR	65.03605	-16.31867	623	16
VADA	64.99487	-16.53817	673	16
VEGG	65.38205	-16.37467	507	16
VONA	64.67131	-17.84279	949	16

Northern Volcanic Zone Network (Sept 2011 to July 2012)

Station	Latitude (º)	Longitude (º)	Elevation (m)	Capacity (Gb)
VVAT	66.03643	-16.85612	132	16
N66D	66.00009	-16.88126	200	16
GUDF	65.91337	-16.96684	321	16
BUNG	65.89703	-16.77482	449	16
KVIH	65.84712	-16.99152	351	8
K008	65.79724	-16.79029	507	16
K006	65.78729	-16.98611	408	4
K030	65.75034	-16.82364	526	4
K010	65.74187	-16.95551	433	4
K025	65.73909	-16.86740	523	4
K050	65.73723	-16.73658	631	8
K071	65.72937	-16.77582	552	16
K055	65.72894	-16.84718	549	16
K110	65.72048	-16.69025	613	4
K115	65.71123	-16.86879	565	16
K120	65.70619	-16.82666	519	16
K190	65.69505	-17.01160	393	16
K200	65.69435	-16.76543	474	4
K170	65.68755	-16.67146	530	4
K219	65.67458	-16.87433	463	4
K250	65.65915	-16.77652	378	16
DRUM	65.60223	-16.83693	384	8
BURF	65.60217	-16.68633	382	16
SKOG	65.57792	-16.50440	402	16
HVAN	65.55409	-16.78980	349	16
TREB	65.52641	-16.82279	450	16
BLAF	65.48870	-16.79785	644	16
SBLA	65.42633	-16.80327	646	8
VEGG	65.38205	-16.37467	507	16
KODA	65.36317	-16.84383	517	16
KOLL	65.29024	-16.56726	593	16
BRUN	65.20461	-16.86597	536	16
HELI	65.19875	-16.21843	491	16
FLAT	65.18279	-16.49796	728	16
HRUR	65.15577	-16.67551	697	16
MYVO	65.15550	-16.36895	639	16
SVAD	65.11746	-16.57498	680	16
TOLI	65.10336	-16.11953	537	8
MIDF	65.08676	-16.32961	572	16
DDAL	65.07739	-16.93341	801	16
DYNG (ask)	65.05194	-16.64806	955	4
HOTT	65.04748	-16.52985	718	16
OSKV	65.03933	-16.70164	1209	16
UTYR	65.03605	-16.31867	623	16
FJAS	65.02470	-17.09217	798	16
VADA	64.99487	-16.53817	673	16
RODG	64.98513	-16.88639	1022	16
MOFO	64.98440	-16.65119	702	16
TOHR	64.91658	-16.78473	715	16
HRIM	64.89633	-16.97921	849	16
LIND	64.85278	-16.45230	726	16
FLUR	64.84354	-17.02693	838	16
KIST	64.79086	-17.36648	1145	4
VONA	64.67131	-17.84279	949	16

Northern Volcanic Zone Network (July 2012 to Sept 2012)

Station	Latitude (º)	Longitude (º)	Elevation (m)	Capacity (Gb)
VIKI	66.07812	-16.82937	58	16
N66D	66.00009	-16.88126	200	ESP
GUDF	65.91337	-16.96684	321	16
KVIH	65.84712	-16.99152	351	8
K006	65.78729	-16.98611	408	16
K050	65.73723	-16.73658	631	8
K250	65.65915	-16.77652	378	ESP
DRUM	65.60223	-16.83693	384	8
HVAN	65.55409	-16.7898	349	16
BLAF	65.4887	-16.79785	644	16
SBLA	65.42633	-16.80327	646	8
VEGG	65.38205	-16.37467	507	16
KODA	65.36317	-16.84383	517	16
KOLL	65.29024	-16.56726	593	ESP
BOTN	65.2183	-16.97939	487	16
BRUN	65.20461	-16.86597	536	16
HELI	65.19875	-16.21843	491	16
FLAT	65.18279	-16.49796	728	16
LOGR	65.15841	-16.82334	730	4
HRUR	65.15577	-16.67551	697	16
MYVO	65.1555	-16.36895	639	16
LOKT	65.13623	-16.91511	630	16
SVAD	65.11746	-16.57498	680	16
TOLI	65.10338	-16.1195	528	ESP
MIDF	65.08676	-16.32961	572	16
VIFE	65.08446	-16.49346	696	4
JONS	65.07747	-16.8057	1174	16
DDAL	65.07739	-16.93341	801	16
KLUR	65.07529	-16.75322	1114	16
ask (DYNG)	65.05194	-16.64806	955	4
HOTT	65.04748	-16.52985	718	16
OSKV	65.03933	-16.70164	1209	16
UTYR	65.03605	-16.31867	623	16
EFJA	65.03358	-16.96212	883	4
FJAS	65.0247	-17.09217	798	16
NAUT	65.02071	-16.5733	692	4
MVET	65.0135	-16.81258	1160	16
KATT	64.99901	-16.96339	885	16
STAM	64.99691	-16.80959	1171	4
VADA	64.99487	-16.53817	673	16
RODG	64.98513	-16.88639	1022	16
MOFO	64.9844	-16.65119	702	16
SSUD	64.94189	-16.85419	807	4
DYSA	64.9349	-16.67546	688	4
TOHR	64.91658	-16.78473	715	16
RIFN	64.91533	-16.37135	989	8
HRIM	64.89633	-16.97921	849	16
LIND	64.85278	-16.4523	726	ESP
FLUR	64.84354	-17.02693	838	ESP
dyn	64.79086	-17.36648	1145	4
KVER	64.76347	-16.61068	829	ESP
VONS	64.67358	-17.75483	???	ESP
ILLA	64.03395	-17.79189	663	16
LAUF	64.02918	-18.13262	563	ESP